Spatially-explicit modeling of modern and Pleistocene runoff and lake extent in the Great Basin region, western United States

Yo Matsubara[1]

Alan D. Howard[1]

[1]Department of Environmental Sciences
University of Virginia
P.O. Box 400123
Charlottesville, VA 22904-4123

Abstract

A spatially-explicit hydrological model balancing yearly precipitation and evaporation is applied to the Great Basin Region of the southwestern United States to predict runoff magnitude and lake distribution during present and Pleistocene climatic conditions. The model iteratively routes runoff through, and evaporation from, depressions to find a steady state solution. The model is calibrated with spatially-explicit annual precipitation estimates and compiled data on pan evaporation, mean annual temperature, and total yearly runoff from stations. The predicted lake distribution provides a close match to present-day lakes. For the last glacial maximum the sizes of lakes Bonneville and Lahontan were well predicted by linear combinations of decrease in mean annual temperature from 0 to 6 °C and increases in precipitation from 0.8 to 1.9 times modern values. Estimated runoff depths were about 1.2 to 4.0 times the present values and yearly evaporation about 0.3 to 1 times modern values.

1. Introduction

The Great Basin of the southwestern United States in the Basin and Range physiographic province contains enclosed basins featuring perennial and ephemeral lakes, playas and salt pans (Fig. 1). The Great Basin consists of the entire state of Nevada, western Utah, and portions of California, Idaho, Oregon, and Wyoming. At present it supports an extremely dry, desert environment; however, about 40 lakes (some reaching the size of present day Great Lakes) episodically occupied the Great Basin, most recently during the last glacial maximum (LGM) [*Snyder and Langbein*, 1962; *Hostetler et al.*, 1994; *Madsen et al.*, 2001]. The Great Basin has been strongly shaped by fluvial erosion, and multiple paleolacustrine deposits and shorelines indicate that the climate has fluctuated greatly during the late Quaternary [*Smith and Street-Perrott*, 1983; *Benson et al.*, 1990; *Oviatt et al.*, 1992].

Lake fluctuation preserved in geologic records in enclosed basins can be a good indicator of climate change [*Benson and Paillet*, 1989; *Menking et al.*, 2003; *Godsey et al.*, 2005], since basin lakes are fed by streams or by overflow from adjacent basin lakes, and they rise and fall in response to changes in a hydrologic balance [*Benson and Paillet*, 1989]. Here we present a high resolution spatially explicit hydrological model that balances runoff resulting from precipitation and lacustrine evaporation to estimate the distribution of lakes under both modern and the late Pleistocene pluvial epoch conditions. Although Pleistocene climate of Great Basin has been studied extensively, spatially explicit modeling of runoff and lake distribution for either modern or LGM period has not been well established. Previous studies either focus on one of the lakes or lake systems in the Great Basin or cover the entire Great Basin at low resolution.

Most of the literature on Pleistocene climate assumes that the Pleistocene conditions can be described as a region-wide change in climatic conditions relative to modern values. However,

Pleistocene precipitation, temperature, evaporation, and runoff may have had somewhat different functional variation with latitude, longitude, and elevation relative to modern conditions. Systematic mismatches between predicted and mapped Pleistocene lakes may be informative of spatial differences in such climatic factors within the Great Basin. The spatially explicit modeling provides a more definitive test of model assumptions and of possible variations in runoff and evaporation during pluvial conditions that cannot be captured by spatially uniform changes in temperature and precipitation [*Knight et al.*, 2001].

The objectives of this study are to 1) test the validity of the newly developed, spatially explicit flow routing model using high resolution elevation data, 2) re-evaluate currently published estimates of late-Pleistocene climatic conditions in Great Basin area, and 3) assess what ranges of environmental conditions best fit the mapped Pleistocene lake distributions. This model is not coupled with an atmospheric climate model to estimate present or Pleistocene climate and resulting lake distributions (e.g., *Hostetler and Giorgi*, 1993; *Giorgi et al.*, 1994; *Clement*, 2005), but rather focuses on what changes in climatic factors relative to the present conditions were required to create the Pleistocene mega-lakes.

1.1 Paleoclimatic conditions

The late Quaternary climate change is believed to have resulted from the expansion of the ice sheet that covered the most of North America [*Manabe and Broccoli*, 1985] and from the relocation of the jet stream responding to the changes in the size of the ice sheet [*Benson and Thompson*, 1987; *Hostetler et al.*, 1994]. Presence of larger ice sheet alone could decrease the surface temperature because of increased surface albedo. Moreover, precipitation and storm tracks generally follow the jet stream under present conditions [*Riehl et al.*, 1954; *Kutzbach and Wright*, 1985], thus the shift in position of the jet stream would have brought colder and wetter

conditions to the Great Basin during the LGM [*Hostetler and Benson*, 1990; *Balch et al.*, 2005], assuming same climatic trend of the jet stream persists. General circulation model (GCM) results show, for time period of about 18 ka, that polar jet stream had split into two branches with southern branch shifting southward as far as 33° N [*Kutzbach and Wright*, 1985]. This southern branch of the polar jet stream gradually shifted back toward north over time, re-merging with the main stream [*Hostetler and Benson*, 1990]. This is evident in the offset of the timing when lakes reached their highstand. Lake Manly and surrounding lakes located at the southern end of the Great Basin reached their highstand between 18 and 16 ka [*Anderson and Wells*, 2003], Lake Lahontan and Lake Bonneville region (mid to northern Great Basin) peaked around 14 to 13 ka [*Enzel et al.*, 2003], and lakes located to the north of Lake Lahontan (e.g. Lake Chewaucan) peaked around 12 ka [*Briggs et al.*, 2005], all of which corresponds well with the shift in the position of the polar jet.

Extensive studies have estimated the climatic conditions that had caused the formation of mega-lakes at Great Basin during the Pleistocene time. Methods utilized for studying paleoclimates include: radiocarbon dating of ostracodes [*Quade et al.*, 2003; *Forester et al.*, 2005] and plant fossils from fossil middens [*Madsen et al.*, 2001], measuring of homogenization temperature of halite inclusions [*Lowenstein et al.*, 1998; *Lowenstein et al.*, 1999], studying of sediment yield rates [*Lemons et al.*, 1996], extracted diatoms, and fossil pollen data from lake sediment cores [*Bradbury*, 1997], and computer modeling such as GCMs [*Gates*, 1976; *Hostetler and Bartlein*, 1990], water balance models [*Wells et al.*, 2003; *Menking et al.*, 2004], and energy balance models [*Benson*, 1981]. The estimated paleoclimatic conditions of the late Quaternary from these studies range widely. Suggested climatic conditions for the LGM period include: evaporation rates that are 0.9 to 0.5 times the present day rate, mean annual temperature (MAT)

of 3 to 15 °C lower than the present MAT, and precipitation that is 0.8 to 2.4 times the present day precipitation [*Galloway*, 1970; *Mifflin and Wheat*, 1979; *Benson*, 1981; *Smith and Street-Perrott*, 1983; *Hostetler and Bartlein*, 1990; *Madsen et al.*, 2001; *Quade et al.*, 2003; *Menking et al.*, 2004]. Some works have proposed as much increase in precipitation as 3.5 to 4.0 times the present day value with 0 to 6.3 °C decrease in MAT [*Lowenstein et al.*, 1998; *Clement*, 2005]. Estimated Pleistocene conditions from various studies are summarized in Table 1.

1.2 Paleolakes of the Great Basin

Three lake systems in Great Basin are commonly used as indicators of the climatic conditions during the LGM: Lake Bonneville (42.4° N 114.3° W, 38.0° N 111.7° W), Lake Lahontan (41.9° N 117.6° W, 38.5° N 120.6° W), and Lake Manly (36.8° N 118.1° W, 35.5° N 115.8° W). This study also focuses on these three lake systems for estimation of paleoenvironments.

Lake Bonneville and Lake Lahontan are the two largest pluvial lakes that occupied the northern Great Basin. Lake Bonneville is the predecessor of the Great Salt Lake that covered as much as 51,000 km^2 when it had reached its highstand elevation of 1552 m (the Bonneville shoreline) [*Lemons et al.*, 1996]. Lake Bonneville overflowed into Snake River from Red Rock Pass, Idaho, stabilizing the lake surface level at the Bonneville shoreline until the catastrophic outflow event of around 14.5- 13.5 ka, which caused the lake surface elevation to lower to 1440 m (the Provo shoreline) [*Oviatt*, 1997]. Great Salt Lake has been stabilized at its current level of approximately 1280 m since ca. 8 ka [*Oviatt et al.*, 2003].

The Lahontan basin is located at western Great Basin, and it is currently occupied by Pyramid Lake, Honey Lake, Walker Lake, and Winnemucca Lake along with several salt flats (e.g. Carson Sink and Humboldt Sink), all of which were part of pluvial Lake Lahontan.

Although there is an evidence of possible overflow from Lake Lahontan to the Snake River during early to mid Pleistocene (1.4 ma, 760 ka) [*Reheis*, 1999], there is no such evidence for the LGM period. Lake Lahontan reached its most recent highstand elevation of 1332 m around 13.8 ka, covering an area of 22,300 km^2.

Lake Manly in Death Valley was the largest of a chain of five lakes that were fed by the Owens and Mojave Rivers, covering approximately 3500 km^2 at one point in its recent history [*Hooke*, 1998; *Anderson and Wells*, 2003]. Lake Manly had reached its maximum highstand about 100,000 years prior to Bonneville and Lahontan highstands, between 180 ka and 120 ka or during Oxygen Isotope Stage (OIS) 6 [*Hooke*, 1998; *Forester et al.*, 2005]. With additional inflow from the Mojave River from the south, the lake reached its highest lake level of 87 m [*Anderson and Wells*, 2003]. During this period, Lake Manly was between 175 to 335 m in depth depending on the post-pluvial sedimentation and uplift rate, since this region has been tectonically active after the desiccation of the lake [*Ku et al.*, 1998; *Lowenstein et al.*, 1999]. Death Valley became relatively wet again after 60 ka, reaching the second highstand period during the LGM. The extent and the duration of the lake during the LGM, however, were much smaller and shorter compared to the OIS 6 highstand. The depth and the surface area of Lake Manly during the LGM were between 80 to 90 m and approximately 1600 km^2, respectively [*Li et al.*, 1997; *Ku et al.*, 1998]. Death Valley has not supported a perennial lake since the desiccation of the Lake Manly around 10 ka.

2 Data and Methods

2.1 Model description

The present hydrologic model is based upon yearly balances of runoff from precipitation and evaporation from lakes. Because large lakes require multi-year changes in this balance to

effect appreciable changes in lake levels, we do not include event-based flow routing. A hydrologic balance for a given enclosed basin can be expressed as:

$$V_O = V_I + (A_T - A_L)P_B R_B + A_L P_L - EA_L \quad (1)$$

where V_O is the yearly volumetric rate of overflow from the basin, V_I is the inflow rate from adjacent basins, A_T and A_L are, respectively, the total basin and lake area, P is the average precipitation rate over the non-lake portion of the basin (subscript B) and directly over the lake (subscript L), R_B is the fraction of precipitation that contributes to runoff, and E is the evaporation rate [*Howard and Matsubara*, 2006]. Hence, any changes in precipitation, evaporation, and/or runoff would cause variations in lake volume and surface area and, possibly, integration or fragmentation of larger basins depending upon whether smaller contributing basins overflow.

Each basin has a maximum lake area (A_{LM}), which is determined by the topography, and any ponding beyond this point would result in an overflow into an adjacent basin. If the calculated A_L (using equation (1) and assuming no overflow to nearby basins) is greater than A_{LM}, then there is an overflow; thus, V_O is calculated by substituting A_{LM} for A_L. An iterative approach is used since overflow from one basin could serve as an inflow into another basin, requiring recalculation of its water balance using equation (1). This iteration continues until there is no change in V_I for any basin. Additional complications arise since two or more overflowing basins may mutually drain, and filling of a downstream basin may submerge the outlet for an upstream basin. In such occurrences the basins are combined into a new sub-basin for subsequent iterations. Model convergence to a steady-state condition is speeded by recalculating the hydrological balance only for sub-basins experiencing changes in V_I during the previous iteration.

Because the model is spatially explicit, both runoff and evaporation need to be estimated for each grid cell. Flow routing also requires construction of a hydrologically sound digital elevation model (DEM). Prediction of runoff is based upon modern yearly runoff at gauging stations within the Great Basin as correlated with estimates of mean annual temperature and precipitation. Evaporation estimates utilize correlations of measured evaporation rates with mean annual temperature and elevation. The following sections describe this model parameterization.

2.2 Data Acquisition and analysis

Many of the data used for this study were obtained from websites, including the digital elevation models (DEMs). All available DEMs are produced by methods that introduce spurious depressions within the landscape [*Soille et al.*, 2003]. Because the model balances evaporation from water within depressions and runoff, these false depressions would result in overestimation of evaporation. A variety of techniques have been developed to remove such spurious depressions [*Martz and Garbrecht*, 1999]. In a landscape with true depressions, such as considered here, care must be taken to distinguish between real and false depressions.

One DEM is available (HYDRO1K, [*Syvitski et al.*, 2005]) that attempts to correct depressions, but we found that this DEM overfilled some depressions and poorly represented the flow network. Our approach has been to utilize grid cells of 1 km^2 dimension generalized from high-resolution DEMs. We utilized 1 arc-second data obtained from the National Elevation Dataset (NED, http://www.seamless.usgs.gov). For our 1-km^2 grid, we utilized the minimum elevation from all NED DEM cells within our coarser grid for flow routing, and the average elevation within the NED cells for estimating precipitation and MAT. To reduce residual false depressions, we replaced each cell with a 3rd order polynomial fit for that cell and the

surrounding 24 cells. Finally, all of depressions smaller than 5 grid cells were infilled, because they are more likely the products of generalization of topography rather than the actual depressions.

Because Lake Bonneville overflowed its basin at about 14.5- 13.5 Ka and eroded its outlet from about 1552 m to 1440 m, we raised the level of the Bonneville basin sill to its pre-overflow level of 1552 m to test the ability of the model to predict basin-full conditions.

Mean annual precipitation data was obtained as a grid format from the National Resources Conservation Services (NRCS, http://ncgc.nrcs.usda.gov/products/datasets/climate/data/precipitation-state). This grid data was created by the PRISM project group from Oregon State University based on precipitation data collected from October, 1961 through December, 1990. Precipitation data from each weather station and DEM were used to interpolate over the entire state. This PRISM interpolation method is beneficial especially for mountainous region, since it incorporates orographic effects on precipitation. After combining precipitation grid for all of the states within the Great Basin, this was also reduced to 1 km per pixel resolution with UTM-zone 11°N projection.

Pan evaporation rate and MAT data along with the deviation from the historical average were provided by the National Climatic Data Center (NCDC, http://www7.ncdc.noaa.gov/IPS/CDPubs?action=getstate). There were 33 stations within the Great Basin that had records of pan evaporation rate, and for each station, pan evaporation rate and latitude, longitude, and elevation of the station were recorded. The actual evaporation is about 70% of the pan evaporation rate [*Kohler et al.*, 1955]; hence the necessary adjustment was made. The mean annual temperature data were available for 309 stations within the Great Basin, and the MAT along with latitude, longitude, and elevation of the station were recorded.

Another data set obtained for this study was mean annual discharge from U.S. Geological Survey (USGS, http://waterdata.usgs.gov/nwis/sw). There were 375 stations that had at least 10 years of recorded data within the Great Basin region, of which 124 stations were discarded due to the location of the gauging stations. Because this region is constantly water limited, many of the stream flows are regulated by dams, reservoirs, and diversions, thus any stations located immediately downstream of such features were discarded. Additionally, 50 stations were excluded because the location of the gauging station could not be matched on our DEM. Such circumstances were determined by comparing the contributing drainage basin area defined by our model and those measured by USGS. When the ratio of the predicted to the measured drainage area was greater than 5 or less than 0.2, the gauging station was eliminated. This could occur, for example, when station is located on a small tributary and was not captured when DEM was generalized. Average mean annual surface runoff values for remaining 201 stations were calculated using the discharge measurements and dividing them by the contributing basin area.

Aside from these climate and hydrological data, a map of current lakes in the Great Basin (revised by Gary Raines, 1996, gb_wb: DDS 41, U.S. Geological Survey, Denver) and map of Pleistocene lakes at the maximum extent (Mifflin, M.D., and Wheat, M.M., 1996, pluvial: DDS 41, U. S. Geological Survey) were obtained from the W.M. Keck Earth Sciences and Mining Research Information Center (http://keck.library.unr.edu/data/gbgeosci/gbgdb.htm). This file was converted from its original ESRI® ArcGIS shapefile format to a grid cell format (zero for no lake, one for a lake) to compare model results to the actual lake distributions.

2.3 Estimation of runoff and evaporation

Producing a hydrological model requires spatially explicit estimates of runoff and evaporation, which we express as functions of precipitation, temperature, latitude, and elevation.

2.3.1 Mean Annual Evaporation Rate

Evaporation is an important component of the hydrologic cycle [*Brutsaert*, 2005] and has a great influence on lake-level fluctuations since it is a primary process for lakes to lose water [*Hostetler and Bartlein*, 1990]. However, evaporation rate is hard to estimate owing to the difficulty of accurately measuring its controlling parameters like wind speed, atmospheric moisture content, and cloud cover [*Shevenell*, 1999].

There are many methods proposed for estimating evaporation, including Penman's equation [*Brutsaert*, 1982]. Penman's equation has been considered to be one of the most reliable equations for estimating evaporation [*Winter et al.*, 1995; *Wu*, 1997; *Hargreaves and Allen*, 2003], and many contemporary studies use Penman's equation as a base, modifying it accordingly to best fit the environment of interest. However, Penman's equation requires many climatic parameters that are not always easily obtainable [*Wu*, 1997; *Shevenell*, 1999]. Weather stations are widely scattered within the Great Basin region, especially in Nevada, and only few of them have records over sufficient periods of time to obtain reliable average values.

A simpler method for estimating evaporation rate was desirable to compensate for paucity of data for the Great Basin region. *Mifflin and Wheat* [1979] found that lake evaporation is dependent on elevation, and consequently on the air temperature. Various equations estimate evaporation rate based on Penman's energy balance equation using only temperature data [*Linacre*, 1977; *Miller and Millis*, 1989; *Shevenell*, 1999; *Hargreaves and Allen*, 2003]. These studies showed that evaporation can be expressed as a function of temperature alone or with latitude and/or elevation. The reliability of these equations have been tested through comparison with the actual pan evaporation measurements or with the estimated results from the original

Penman's equation [*Wu*, 1997]. *Wu* [1997] concludes that evaporation rate can be sufficiently estimated by temperature data only.

In order to estimate evaporation, the MAT was first estimated. A multiple regression analysis was conducted using the Microsoft® Excel to express the MAT (°F) as a function of latitude (*lat*: in decimal degree), longitude (*lon*: in decimal degree) and elevation (*EL*: in m):

$$MAT = 141.545 - 1.588lat - 0.00873EL + 0.173lon \qquad (R^2 = 0.86,\ n = 309). \quad (2)$$

We utilized Fahrenheit for our MAT units simply to keep the coefficients small and to avoid the mathematical complexity associated with zero and negative MAT values in estimating equations.

Following the works of *Linacre* [1977] and *Shevenell* [1999] and using the evaporation rate adjusted for lake evaporation and estimated MAT from above equation, a multiple linear regression analysis was conducted to express the mean annual evaporation rate, *E*, as a function of MAT (°F) and elevation (m):

$$E = -2.49 + 0.00033EL + 0.062MAT \qquad (n = 33,\ R^2 = 0.77). \quad (3)$$

It should be noted that elevation used to calculate MAT and evaporation is the average elevation of the lake surface, which fluctuates with changes in lake level. This allows evaporation rate to change accordingly with lake level since increase in lake level would cause evaporation rate to decrease. It should also be noted that pan evaporation rates we utilized are for fresh water. Many of the lakes in the Great Basin have high salinity, thus evaporation rates estimated by equation (3) could be overestimated.

2.3.2 Mean Annual Runoff

Surface runoff occurs as a response to the precipitation, and it is sensitive to variations in precipitation inputs, evaporation, and topography [*Mifflin and Wheat*, 1979; *Haddeland et al.*, 2002]. Our aim for choosing methods for estimating climatic and hydrologic parameters was to

keep the relationship as generalized and simple as possible. While a number of methods are used for runoff estimation [*U.S. Soil Conservation Service*, 1986; *Knight et al.*, 2001; *Ferguson* 1996], many of them were developed mainly for agricultural and city planning purposes and are more appropriate for estimating runoff for small localized areas where specific soil types and land covers are known and somewhat uniform. The Great Basin is too large a region to apply area-specific methods.

Schumm [1965] suggested that mean annual runoff can be expressed as a function of precipitation and temperature. His graph of mean annual precipitation against mean annual runoff for different weighted MAT for entire United States clearly showed a strong relationship between runoff, MAT, and precipitation. This graph was later modified by *Mifflin and Wheat* [1979] for Nevada, where annual precipitation is considerably lower than rest of the regions in the United States. This method can be regarded (at least under present day conditions) to include implicitly the effects of soil and land cover types, since gauging stations measures discharges that resulted under the influence of soils and land cover [*Schumm*, 1965].

Following the studies of *Schumm* [1965] and *Mifflin and Wheat* [1979], mean annual runoff (R: in m yr^{-1}) was expressed as a function of annual precipitation (P: in m yr^{-1}) and MAT (°F). However, using discharge data from a gauging station to estimate the surface runoff for every grid cell within its contributing area upstream of the station may lead to a biased estimation. Therefore, we utilized surface runoff, precipitation, and MAT that were averaged over each contributing drainage basin. To estimate average surface runoff, we first conducted a regression analysis using the surface runoff, precipitation, and MAT measured at or estimated for the gauging station. Using the resultant relationship, surface runoff was estimated for each grid

cell, which was then used to calculate the average surface runoff for each drainage basin. The equation we used in our model for surface runoff estimation is as follows:

$$R = 38871.17P^{2.11}MAT^{-3.08} \qquad (n = 201, R^2 = 0.64) \qquad (4)$$

3 Application to modern and Pleistocene conditions

The model was first validated by applying it to the present day Great Basin. Proposed Pleistocene ice age conditions are usually expressed as a relative change from the present conditions, thus each equation (2, 3, and 4) was scaled accordingly to simulate the Pleistocene conditions. For example, *Menking et al.* [2004] proposed that precipitation was 2.4 times the present precipitation during the LGM, and to simulate under this condition, modern precipitation values were simply multiplied by 2.4.

Equation (3) shows that any changes in MAT would also change evaporation rate in our model. For our simulations, it was assumed that changes in evaporation rate occur only as a result of changes in MAT. Evaporation is sensitive to temperature, and while other controlling factors such as cloud cover, wind speed, and humidity are not well studied for pluvial period, paleotemperatures have been quantified by distributions of fossil species, isotopic signatures, and tree lines. Nevertheless, evaporation rate change due to increased cloud cover could always be included by further reducing the evaporation rate independent of temperature change.

4 Results

4.1 Present day Great Basin

Using our DEM with the grid-based precipitation map and estimation of runoff and evaporation from equations 2-4, the flow routing model reproduced the modern spatial distribution and size of lakes reasonably well (Fig. 2). Most of the basin lacked lakes as

anticipated, and most of the larger lakes, including the Great Salt Lake, Pyramid Lake, Honey Lake, and Lake Tahoe, were well predicted. Predicted lake surface area for these lakes matched closely with the actual surface area (Table 2). It should be noted that the Great Salt Lake was slightly underestimated by our model (Fig. 2). This could be due to the high salinity of the Great Salt Lake [*Miller and Millis*, 1989; *Grayson*, 1993], which would reduce the evaporation rate.

Overall, there are more lakes predicted by our model than those actually mapped. This can be partially attributed to the fact that this region is constantly water limited, thus water withdrawals, regulations of the flow, and damming of the rivers for agricultural and industrial purposes are often practiced [*Grayson*, 1993]. This would cause the stream flow and water ponding not reflective of the natural climatic controls, such as precipitation, evaporation, and temperature. For example, Owens Lake was much deeper and larger than the present before agricultural irrigation started in 1912 [*Smith and Street-Perrott*, 1983]. When compared to the USGS hydrologic unit map for the Great Basin region [*Plume and Carlton*, 1988], some of the lakes over predicted by the model were actually indicated as a reservoir. The base map we utilized for comparing the simulated result with did not include reservoirs, causing the result to be classified as mismatched. Also, we have reduced the resolution of the DEM to 1 km^2 pixel, and the generalization procedure could create imaginary depressions (false topography).

4.2 LGM Great Basin

A series of simulations were conducted to find what combination of changes in MAT and precipitation best fit the mapped Pleistocene lake distributions. Our model resulted in lake distributions that were generally consistent with the mapped Pleistocene paleoshorelines, though maximum extent of late Pleistocene lakes at the northern half and southern half of the Great Basin could not be simultaneously produced by the same proportional changes in MAT and

precipitation (Fig. 3a and b). Lake Manly in the southern region could not be predicted whenever conditions were set to fit the two large northern lakes, Lake Bonneville and Lake Lahontan (Fig 3a). Conversely, when conditions were set to fit for Lake Manly, Lake Lahontan and Lake Bonneville regions were overestimated (Fig 3b). Table 3 summarizes observed and simulated lake surface elevation and surface area.

As for Lake Manly, we first set the conditions so that resultant extent would match the mapped shoreline. The predicted lake was about 3170 km^2 in size and reached the elevation of 85.7 m. This is comparable to the maximum highstand known for Lake Manly (lake surface area of 3500 km^2 and elevation of 87 m), which occurred during OIS 6 [*Hooke*, 1998; *Forester et al.*, 2005]. We also predicted Lake Manly during the LGM, which had a surface area of 1600 km^2 and a depth of about 80 to 90 m [*Li et al.*, 1997; *Ku et al.*, 1998]. We found sets of conditions that would result in Lake Manly with surface area and depth that match LGM highstand level (Fig. 4, 5).

We estimated conditions necessary to produce the observed Pleistocene lakes expressed in two ways: 1) combinations of changes in average runoff and evaporation and 2) combinations of changes in precipitation and MAT. The former is less model-dependent, since unlike the second method, it does not assume present spatial patterns of runoff and evaporation variation to change proportionally during the Pleistocene conditions. They were obtained, rather, as a result of MAT and precipitation changes.

Figure 4 illustrates that the changes in surface runoff (R) can be expressed as a linear function of changes in evaporation rate (E). Expressions for Lake Bonneville, Lake Lahontan, and Lake Manly (OIS 6) from the simulations are, respectively,

$$R = 0.32E - 0.02,$$
$$R = 0.31E - 0.04, \text{ and}$$
$$R = 0.24E - 0.02.$$

The simulations indicate that in order to have adequate size lakes in the Great Basin, surface runoff must be increased by factor of 1.2 to 6.0 for evaporation rates in the range of 0.4 to 1.5 m yr^{-1}. This is reasonable magnitude of increase since it has been proposed that the flow in the Manly system during the LGM was at least 3.5 times greater than that of the present day [*Smith and Street-Perrott*, 1983]. It can be inferred that a greater combination in increase in runoff and decrease in evaporation is required for Lake Manly (both LGM and OIS 6 lake levels) relative to lakes Bonneville and Lahontan (Fig. 4).

Our model resulted in multiple possible combinations of precipitation and MAT changes that can result in the lake distributions that agree with mapped paleoshorelines (Fig. 5). This graph also shows that conditions required to form lakes at northern (Bonneville/ Lahontan region) and southern (Manly region) Great Basin were different. The southern half of the Great Basin requires greater precipitation change and/or temperature change than northern lakes. Our parameter values producing the observed Pleistocene lakes are within the range of previously proposed conditions, though specific combinations may be different than previously proposed (cf. Table 1 and Figure 4). For instance, some studies have suggested about 5 to 8 °C decrease in MAT along with the precipitation increase by factor of 2.4 to 2.6 as required conditions to form Lake Lahontan [*Thompson et al.*, 1999], while our model needed 1.0 to 1.6 times the present precipitation for same range of MAT change.

5 Discussion

Our results indicate that Lake Manly region required greater changes in runoff, evaporation rate, precipitation, and/or temperature compared to the Lake Bonneville/ Lahontan

region. One possible explanation for this difference may be that, the polar jet stream had greater effects to the southern Great Basin than to the northern Great Basin. The difference in the effect of jet stream between the two regions could be attributed to the topography of the western United States. The Sierra Nevada is a mountain range that trends north-south from 40 to 35 °N and is located at the western border of the Great Basin. At present, this mountain range along with another north-south trending Cascades Mountain Range located to the north blocks greater part of the winds coming in from the Pacific Ocean and causes all of the moisture to precipitate to the west of the mountain range [*Antevs*, 1952]. The Sierra Nevada also blocks cold waves from reaching the Great Basin area [*Antevs*, 1952]. To the south of Sierra Nevada is the Mojave Desert, which is relatively flat region with few mountains trending east-west. When the wind from the west encounter the Sierra Nevada and the Cascade mountain range, wind detours south around the Sierra Nevada flowing inland through the Mojave Desert [*Bryson and Hare*, 1974]. Around 20 to 18 ka, polar jet had shifted south of Sierra Nevada (~ 33 °N) [*Kutzbach and Wright*, 1985], and during this time, the jet stream would have flown directly inland through Mojave Desert region toward Great Basin. Precipitation is most closely associated with the jet stream today and its maxima tend to be oriented along or just north of the jet stream [*Riehl et al.*, 1954]. Therefore, when the jet stream was located over the Mojave region, Lake Manly could have experienced fuller impact of the polar front.

Another possible source of water contributing to the southern region is groundwater flow (J. Quade, personal communications, 2006). Death Valley receives groundwater flow primarily from Spring Mountain near Las Vegas, Nevada [*Hunt*, 1975; *Prudic et al.*, 1995; *Plume*, 1996; *D'Agnese et al.*, 1997; *Li et al.*, 1997], and the core sample from Death Valley includes deposits with high concentration of Ca-rich minerals, indicating that groundwater inflow had often played

an important role over its history [*Li et al.*, 1997; *Anderson and Wells*, 2003]. Currently groundwater flow is not considered in our model and any excess water (relative to the amount needed for Lake Lahontan) that is needed to create the Lake Manly maximum might be attributable to such flow.

Our model results also shows that slightly greater changes in runoff, evaporation rate, precipitation, and/or temperature were required for Lake Bonneville than Lake Lahontan region. Presence of large lakes can affect local climate. Evaporation from the lake surface adds moisture to the air, which could be recycled back to the lake as precipitation. Lake Bonneville may have had localized increase in precipitation due to the moisture added to the air from Lake Bonneville itself and also from Lake Lahontan located to the west [*Hostetler et al.*, 1994]. However, the differences in conditions between the two lakes are very small, thus it could be the result of generalization of the DEM.

In our model, evaporation decreases as MAT decreases. Decreasing the MAT by 9 °C for northern lakes or 13 °C for southern lake would reduce the evaporation rate, on average, to 0.01 times the modern day rate. This would place a constraint on range of possible change in MAT, and it is suggested that MAT during the LGM was at the most 9 to 13 °C colder than the present time.

It should be also noted that currently, northern Great Basin is approximately 4.3 to 4.6 °C colder than the southern Great Basin on average. Temperature of the region adjacent to the ice sheet would be colder than the region further south [*Gates*, 1976; *Kutzbach and Wright*, 1985], hence it is likely that some temperature gradient existed within the Great Basin during the LGM as well. This implies that the MAT for the southern Great Basin region can not be more than 4.3 °C lower than that for the northern Great Basin.

6 Conclusions

Overall, our simple parameterized model was able to replicate the extent and spatial distributions of Pleistocene lakes based upon proportional changes in mean annual precipitation and MAT. The sizes of lakes Bonneville and Lahontan were well predicted by linear combinations of decrease in MAT from 0 to 6 °C and change in mean annual precipitation from 0.8 to 1.9 times modern values. To produce the late Pleistocene size of Lake Manly, however, combinations of MAT decrease up to 10 °C or precipitation increase up to 2.5 times modern values are required. Possible explanations for this latitudinal difference in estimated climate include groundwater contributions to Lake Manly that we had not included or spatially non-uniform climate and vegetation change in consequence to the positioning of the jet stream and the topography.

The estimated changes in mean annual precipitation and MAT (or alternatively runoff and evaporation) are within previous estimates. Moreover, our model was able to replicate adequate sized pluvial lakes with smaller magnitude of changes than many of the previous studies.

Our flow routing model was not coupled with atmospheric climate model for this study. Thus we cannot directly simulate the changes in temperatures, cloud cover, wind patterns, and precipitation and their effects upon evaporation and runoff. However, the flow model could be incorporated into more advanced climate and runoff modeling coupled to GCMs, and could be simulated under more specific treatment of seasonality and vegetation influences. The flow routing program is available from the second author (A.D. Howard).

References

Anderson, D.E., and S.G. Wells (2003), Latest Pleistocene lake highstands in Death Valley, California, in *Paleoenvironments and paleohydrology of the Mojave and southern Great Basin deserts*, edited by Y. Enzel, S.G. Wells, and N. Lancaster, pp. 115-128, The Geological Society of America, Colorado.

Antevs, E. (1952), Cenozoic climates of the Great Basin, *Geologische Rundschau*, *40* (94-108).

Balch, D.P., A.S. Cohen, D.W. Schnurrenberger, B.J. Haskell, B.L.V. Garces, J.W. Beck, H. Cheng, and R.L. Edwards (2005), Ecosystem and paleohydrological response to Quaternary climate change in the Bonneville Basin, Utah, *Palaeogeography, Palaeoclimatology, Palaeoecology*, *221*, 99-122.

Benson, L.V. (1981), Paleoclimatic significance of lake-level fluctuations in the Lahontan basin, *Quaternary Research*, *16* (3), 390-403.

Benson, L.V., D.R. Currey, R.I. Dorn, K.R. Lajoie, C.G. Oviatt, S.W. Robinson, G.I. Smith, and S. Stine (1990), Chronology of expression and contraction of four Great Basin lake systems during the past 35,000 years Paleoclimates; the record from lakes, ocean and land, *Palaeogeography, Palaeoclimatology, Palaeoecology*, *78* (3-4), 241-286.

Benson, L.V., and F.L. Paillet (1989), The use of total lake-surface area as an indicator of climatic change: examples from the Lahontan basin, *Quaternary Research*, *32*, 262-275.

Benson, L.V., and R.S. Thompson (1987), Lake-level variation in the Lahontan basin for the past 50,000 years, *Quaternary Research*, *28*, 69-85.

Bradbury, J.P. (1997), A diatom record of climate and hydrology for the past 200 ka from Owens Lake, California with comparison to other Great Basin records, *Quaternary Science Reviews*, *16*, 203-219.

Briggs, R.W., S.G. Wesnousky, and K.D. Adams (2005), Late Pleistocene and late Holocene lake highstands in the Pyramid Lake subbasin of Lake Lahontan, Nevada, USA, *Quaternary Research*, *64*, 257-263.

Brutsaert, W. (1982), *Evaporation into the atmosphere*, 299 pp., Kluwer Academic Publishers, Dordrecht.

Brutsaert, W. (2005), *Hydrology - an Introduction*, 605 pp., Cambridge University Press, Cambridge.

Bryson, R.A., and F.K. Hare (1974), The Climates of North America, in *The Climates of North America*, edited by R.A. Bryson, and F.K. Hare, pp. 1- 47, American Elsevier Publishing Company, Inc, New York.

Clement, S.M. (2005), Modeling of the Great Basin pluvial lakes during the Last Glacial Maximum, Kent State University, Kent.

D'Agnese, F.A., C.C. Faunt, A.K. Turner, and M.C. Hill (1997), Hydrogeologic evaluation and numerical simulation of the Death Valley regional ground-water flow system, Nevada and California, *U. S. Geological Survey, Water-Resources Investigations Report, 96-4300*, 1-124.

Enzel, Y., S.G. Wells, and N. Lancaster (2003), Late Pleistocene lakes along the Mojave River, southeast California, in *Paleoenvironments and paleohyfrology of the Mojave and southern Great Basin deserts*, edited by Y. Enzel, S.G. Wells, and N. Lancaster, pp. 61 - 77, Colorado.

Ferguson, B.K. (1996), Estimation of direct runoff in the Thornthwaite water balance, *Professioinal Geographer*, *48* (3), 263-271.

Forester, R.M., T.K. Lowenstein, and R. Spencer (2005), An ostracode based paleolimnologic and paleohydrologic history of Death Valley: 200 to 0 ka, *Geological Society of America Bulletin*, *117* (11/12), 1379-1386; doi:10.1130/B25637.1.

Galloway, R.W. (1970), The full-glacial climate in the southwestern United States, *Annals of the Association of American Geographers*, *60* (2), 245-256.

Gates, W.L. (1976), Modeling the ice-age climate, *Science*, *191*, 1138-1144.

Giorgi, F., S.W. Hostetler, and C.S. Brodeur (1994), Analysis of the surface hydrology in a regional climate model, *Quarterly Journal - Royal Meteorological Society*, *120* (515), 161-183.

Godsey, H.S., D.R. Currey, and M.A. Chan (2005), New evidence for an extended occupation of the Provo shoreline and implications for regional climate change, Pleistocene Lake Bonneville, Utah, USA, *Quaternary Research*, *63*, 212-223.

Grayson, D.K. (1993), *The desert's past: A natural prehistory of the Great Basin*, 3569 pp., Smithsonian Institution, Washington D.C.

Haddeland, I., B.V. Matheussen, and D.P. Lettenmaier (2002), Influence of spatial resolution on simulated streamflow in a macroscale hydrologic model, *Water Resources Research*, *38* (7), 10.1029/2001WR000854.

Hargreaves, G.H., and R.G. Allen (2003), History and evaluation of Hargreaves evaptranpiration equation, *Journal of Irrigation and Drainage Engineering*, *129* (1), 53-63.

Hooke, R.L. (1998), Did Lake Manly overflow at Ash Hill?, *Earth Surface Processes and Landforms*, *23* (4), 377-384.

Hostetler, S.W., and P.J. Bartlein (1990), Simulation of lake evaporation with application to modeling lake level variations of Harney-Malheur Lake, Oregon, *Water Resources Research*, *26* (10), 2603-2612.

Hostetler, S.W., and L.V. Benson (1990), Paleoclimatic implications of the high stand of Lake Lahontan derived from models of evaporation and lake level, *Climate dynamics*, *4*, 207-217.

Hostetler, S.W., and F. Giorgi (1993), Use of output from high-resolution atmospheric models in landscape- scale hydrologic models: an assessment, *Water Resources Research*, *29* (6), 1685-1695.

Hostetler, S.W., F. Giorgi, G.T. Bates, and P.J. Bartlein (1994), Lake-atmosphere feedbacks associated with paleolakes Bonneville and Lahontan, *Science*, *263*, 665-668.

Howard, A.D., and Y. Matsubara (2006), Flow routing in a cratered landscape: 1. Background and application to Mars, *Lunar and Planetary Sci. Conf. XXXVII*, Abstract.

Hunt, C.B. (1975), *Death Valley: geology, ecology, archaeology*, 234 pp., University of California Press, Berkeley.

Knight, C.G., H. Chang, M.P. Staneva, and D. Kostov (2001), A simplified basin model for simulating runoff: the Struma River GIS, *Professioinal Geographer*, *53* (4), 533-545.

Kohler, M.A., T.J. Nordenson, and W.E. Fox (1955), Evaporation from pans and lakes, in *Research paper*, pp. 1-21, U.S. Department of Commerce (Weather Bureau), Washington D.C.

Ku, T.L., S. Luo, T.K. Lowenstein, J. Li, and R. Spencer (1998), U-series chronology of lacustrine deposits in Death Valley, California, *Quaternary Research*, *50*, 261-275.

Kutzbach, J.E., and H.E. Wright, Jr. (1985), Simulation of the climate of 18,000 years BP: Results for the North American/ North Atlantic/ European sector and comaprison with the geologic record of North America, *Quaternary Science Reviews*, *4*, 147-187.

Lemons, D.R., M.R. Milligan, and M.A. Chan (1996), Paleoclimatic implications of late Pleistocene sediment yield rates for the Bonneville Basin, northern Utah, *Palaeogeography, Palaeoclimatology, Palaeoecology*, *123*, 147-159.

Li, J., T.K. Lowenstein, and I.R. Blackburn (1997), Responses of evaporite mineralogy to inflow water sources and climate during the past 100 ky in Death Valley, California, *Geological Society of America Bulletin*, *109* (10), 1361-1371.

Linacre, E.T. (1977), A simple formula for estimating evaporation rate in various climates, using temperature data alone, *Agricultural Meteorology*, *18*, 409-424.

Lowenstein, T.K., J. Li, and C.B. Brown (1998), Paleotemperatures from fluid inclusions in halite: method verification and a 100,000 year paleotemperature record, Death Valley, CA, *Chemical Geology*, *150*, 223-245.

Lowenstein, T.K., J. Li, C.B. Brown, S.M. Roberts, T.-L. Ku, S. Luo, and W. Yang (1999), 200 k.y. paleoclimate record from Death Valley salt core, *Geology*, *27* (1), 3-6.

Madsen, D.B., J.M. Broughton, S.D. Livingston, J. Hunt, J. Quade, D.N. Schmitt, I.M.W. Shaver, D. Rhode, and D.K. Grayson (2001), Late Quaternary environmental change in the Bonneville basin, western USA, *Palaeogeography, Palaeoclimatology, Palaeoecology*, *167* (3-4), 243-271.

Manabe, S., and A.J. Broccoli (1985), The influence of continental ice sheets on the climate of an ice age, *Journal of Geophysical Research*, *90*, 2167-2190.

Martz, L.W., and J. Garbrecht (1999), An outlet breaching algorithm for the treatment of closed depressions in a raster DEM, *Computers & Geosciences*, *25*, 835- 844.

Menking, K.M., R.Y. Anderson, N.G. Shafike, K.H. Syed, and B.D. Allen (2004), Wetter or colder during the Last Glacial Maximum? Revisiting the pluvial lake question in southwestern North America, *Quaternary Research*, *62*, 280-288.

Menking, K.M., K.H. Syed, R.Y. Anderson, N.G. Shafike, and J.G. Arnold (2003), Model estimates of runoff in the closed, semiarid Estancia basin, central New Mexico, USA, *Hydrological Sciences*, *48* (6), 953-970.

Mifflin, M.D., and M.M. Wheat (1979), Pluvial lakes and estimated pluvial climates of Nevada, in *Nevada Bureau of Mines and Geology Bulletin*, Mackay School of Mines, University of Nevada, Reno.

Miller, W., and E. Millis (1989), Estimating evaporation from Utah's Great Salt Lake using thermal infrared satellite imagery, *Water Resources Bulletin*, *25* (3), 541-550.

Oviatt, C.G. (1997), Lake Bonnecille fluctulations and global climate change, *geology*, *25* (2), 155- 158.

Oviatt, C.G., D.R. Currey, and D. Sack (1992), Radiocarbon chronology of Lake BOnneville, Eastern Great Basin, USA, *Palaeogeography, Palaeoclimatology, Palaeoecology*, *99*, 225-241.

Oviatt, C.G., D.B. Madsen, and D.N. Schmitt (2003), Late Pleistocene and early Holocene rivers and wetlands in the Bonneville basin of western North America, *Quaternary Research*, *60*, 200-210.

Plume, R.W. (1996), Hydrogeologic framework of the Great Basin Region of Nevada, Utah, and adjacent states, *U. S. Geological Survey Professional Paper*, *1409-B*, B1-B64.

Plume, R.W., and S.M. Carlton (1988), Hydrogeology of the Great Basin region of Nevada, Utah, and adjacent states, US Geological Survey, Reston, Va.

Prudic, D.E., J.R. Harrill, and T.J. Burbey (1995), Conceptual evaluation of regional ground-water flow in the carbonate-rock province of the Great Basin, Nevada, Utah, and Adjacent States, *U. S. Geological Survey Professional Paper, 1409-D*, D1-D102.

Quade, J., R.M. Forester, and J.F. Whelan (2003), Late Quaternary paleohydrologic and paleotemperature change in southern Nevada, in *Paleoenvironments and paleohydrology of the Mojave and southern Great Basin deserts*, edited by Y. Enzel, S.G. Wells, and N. Lancaster, pp. 165-188, THe Geological Society of America, Inc., Colorado.

Reheis, M. (1999), Highest pluvial-lake shorelines and Pleistocene climate of the western Great Basin, *Quaternary Research, 52*, 196-205.

Riehl, H., M.A. Alaka, C.L. Jordan, and R.J. Renard (1954), The Jet Stream, *Meteorological Monographs, 2* (7), 38- 47.

Schumm, S.A. (1965), Quaternary Paleohydrology, in *The Quaternary of the United States*, edited by H.E. Wright, Jr., and D.G. Frey, pp. 783-794, Princeton University Press.

Shevenell, L. (1999), Regional potential evapotranspiration in arid climates based on temperature, topography and calculated solar radiation, *Hydrological Processes, 13*, 577-596.

Smith, G.I., and F.A. Street-Perrott (1983), Pluvial lakes of the western United States, in *The late Pleistocene*, edited by S.C. Porter, pp. 190-212, University of Minnesota Press, Minneapolis.

Snyder, C.T., and W.B. Langbein (1962), The Pleistocene lake in Spring Valley, NEvada, and its climatic implications, *Journal of Geophysical Research, 67*, 2385-2394.

Soille, P., J. Vogt, and R. Colombo (2003), Carving and adaptive drainage enforcement of grid difital elecation models, *Water Resources Research, 39* (12), 1366.

Syvitski, J., A.J. Kettner, S.D. Peckham, and S.J. Kao (2005), Predicting the flux of sediment to the coastal zone: Application to the Lanyang Watershed, Northern Taiwan, *J. Coast. Res., 21* (3), 580- 587.

Thompson, R.S., K.H. Anderson, and P.J. Bartlein (1999), Quantitative paleoclimatic reconstructions from late Pleistocene plant macrofossils of the Yucca Mountain region, in *U.S. Geological Survey Open-File Report*, U.S. Geological Survey.

U.S. Soil Conservation Service (1986), Urban hydrology for small watersheds, in *Technical Release*, U.S. Soil COnservation Service, Washington DC.

Wells, S.G., W.J. Brown, Y. Enzel, R.Y. Anderson, and L.D. McFadden (2003), Late Quaternary geology and paleohydrology of pluvial Lake Mojave, southern California, in *Paleoenvironments and paleohydrology of the Mojave and southern Great Basin desert*, edited by Y. Enzel, S.G. Wells, and N. Lancaster, pp. 79 - 114, The Geological Society of America, Colorado.

Winter, T.C., D.O. Rosenberry, and A.M. Sturrock (1995), Evaluation of 11 equations for determining evaporation for a small lake in the north central United States, *Water Resources Research, 31* (4), 983-993.

Wu, I.-P. (1997), A simple evapotranspiration model for Hawaii: the Hargreaves Model, in *Engineer's Notebook*, pp. 2, Cooperative Extension service, Manoa.

Tables and Figures

Table 1. Summary of previously proposed climatic conditions for Great Basin during the LGM. Change in precipitation and evaporation is expressed as a ratio of LGM conditions to present conditions.

Location	Δ MAT (°C)	Δ P (LGM/present)	Δ E	Method	Reference
Lake Bonneville	-13*	1	-	GCM	Hostetler et al., 1994
Lake Bonneville	-13	1.2 - 1.3	-	sediment yield rate	Lemons et al., 1996
Spring Lake	-	1.66	0.7	hydrologic balance model	Snyder & Longbein, 1962
Lake Lahontan	-3	1.5 - 1.80 (ave 1.65)	0.9	mass balance model	Mifflin & Wheat, 1979
Lake Lahontan	n/a	1.8	0.58	thermal evap model	Hostetler & Benson, 1990
Lake Lahontan	-14*	1	-	GCM	Hostetler et al., 1994
Lake Manly	-4 to -15 **	wetter	-	halite inclusion	Lowenstein et al., 1998, 1999
Yucca Mountain	-5.5 to -8	2.4 - 2.6	-	packrat middens	Thompson et al., 1999
Yucca Mountain	-7.5	2.4	-	packrat middens	Menking et al., 2004
Southwestern US	-10 to -11	0.8 - 0.9	0.5	depostis, tree lines, pollen	Galloway, 1970
Great Basin	-2.5 to -3	1.5 -2.0	-	hydrologic balance model	Antevs, 1952
Great Basin	-10	1.7	0.9 - 0.55	hydrologic balance model	Smith & Street-Perrot 1983
Mojave (Southern CA)	- 7	-	-	O, C dating	Quade et al., 2003
Sierra Nevada	-6	1.2 - 1.4	-	energy and water balance models	Menking et al., 2004

* July temperature; ** Spring temperature

Table 2. Comparison of actual (observed) and simulated lake surface area under present day conditions.

System	Lake Name	Lake Surface Area (km^2)		Reference*
		Observed	Simulated	
Bonneville	Great Salt Lake	2460 - 8547	7464	1
	Utah Lake	392	353	2
	Sevier Lake	486.9	1860	3
Lahontan	Honey Lake	233	477	4
	Pyramid Lake	453	671	5
	Walker Lake	148	6	4
	Lake Tahoe	499	597	5
Manly	Death Valley	-	9	
	Owens Lake	249	560	4
	Mono Lake	180	633	5
	Searles Lake	-	11	

*References: 1. USGS websites; 2. Utah department of Environmental quality (Utah division of water quality) website; 3. Utah State University department of engineering website; 4. Calculated using ArcGIS (data provided by W.M. Keck Earth Sciences and Mining Research Information Center); 5. International Lake Environment Committee Foundation website

Table 3. Comparison of actual (observed) and simulated lake surface levels and surface areas for LGM.

	Lake Name	LGM Lake Level (m)			Lake Surface Area (km^2)		Reference*
		Observed	Simulated	Difference	Observed	Simulated	
1	**Bonneville**	1552	1552	0	51,000	52,882	
2	Clover	1730	1753	23	911.7	1235	1, 3
3	Diamond	1829	1800.1	-28.9	1015.3	899	1, 3
4	Franklin	1850	1860.5	10.5	1251.0	1415	1, 3
5	Gale	1905	1908.8	3.8	411.8	342	1, 3
6	Hubbs	1920	1868.1	-51.9	505.1	272	1, 3
7	Jakes	1945	1932.2	-12.8	163.2	122	1, 3
8	Newark	1847	1798.7	-48.3	782.2	518	1, 3
9	Railroad	1484	1444.5	-39.5	971.3	526	1, 3
10	Spring	1759	1763.3	4.3	603.5	1084	1, 3
11	Waring	1761	1779.4	18.4		1807	1
12	**Lahontan**	1332	1334.3	2.3	22,300	25,233	
13	Desatoya	1899	1859.4	-39.6	435.1	417	1, 3
14	Dixie	1097	1034.3	-62.7	714.8	244	1, 3
15	Edwards	1609	1562.3	-46.7	264.2	301	1, 3
16	Tahoe	1926	1914.3	-11.7	529.0	629	1, 3, 4
17	Toiyabe	1702	1709.8	7.8	525.8	1125	1, 3
18	Wellington	1475	1404.2	-70.8	303.0	61	1, 3
19	**Manly**	87	88.4	1.41	3500	3169	
20	China	695	687.2	-7.76	277.9	1133	2, 4
21	Owens	1146	1146.8	0.8	543.2	720	2, 4
22	Panamint	602	597.9	-4.12	809.8	924	2, 4
23	Russell	2155	2174.7	19.7	818.4	976	1, 2, 3
24	Searles	695	687.2	-7.76	615.0	1133	2, 4

*Reference: 1. USGS Map of Pluvial Lake in Nevada (Reheis, 1999); 2. Benson et al., 1990; 3. Mifflin and Wheat, 1979; 4. Calculated using ArcGIS (data provided by W.M. Keck Earth Sciences and Mining Research Information Center).

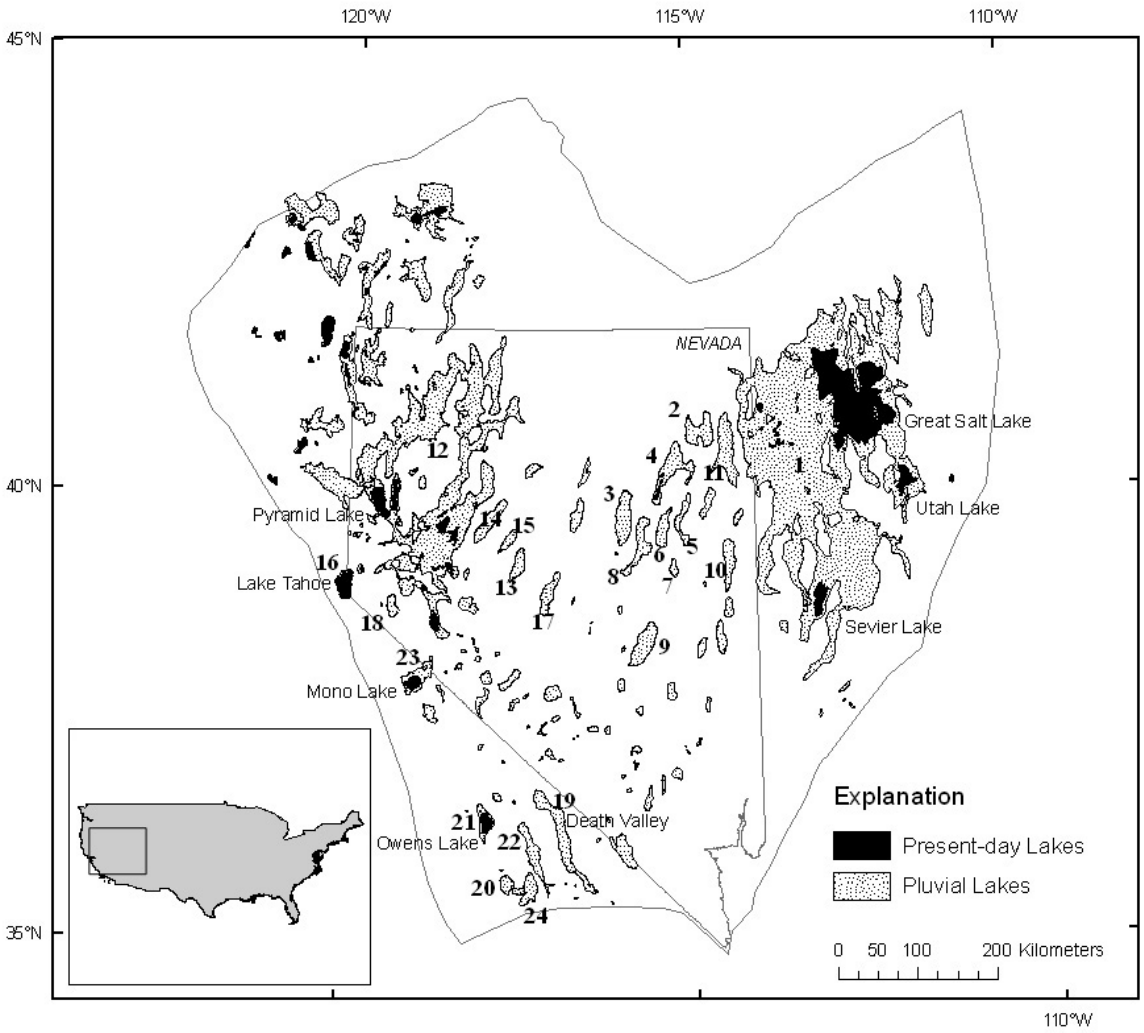

Figure 1. Present and pluvial lakes at their maximum known extent reached during late Pleistocene within Great Basin. Pluvial Lakes are numbered according to table 3. Note that few of the present lakes are the same size as pluvial lakes. An outline of Nevada is shown as a location indicator.

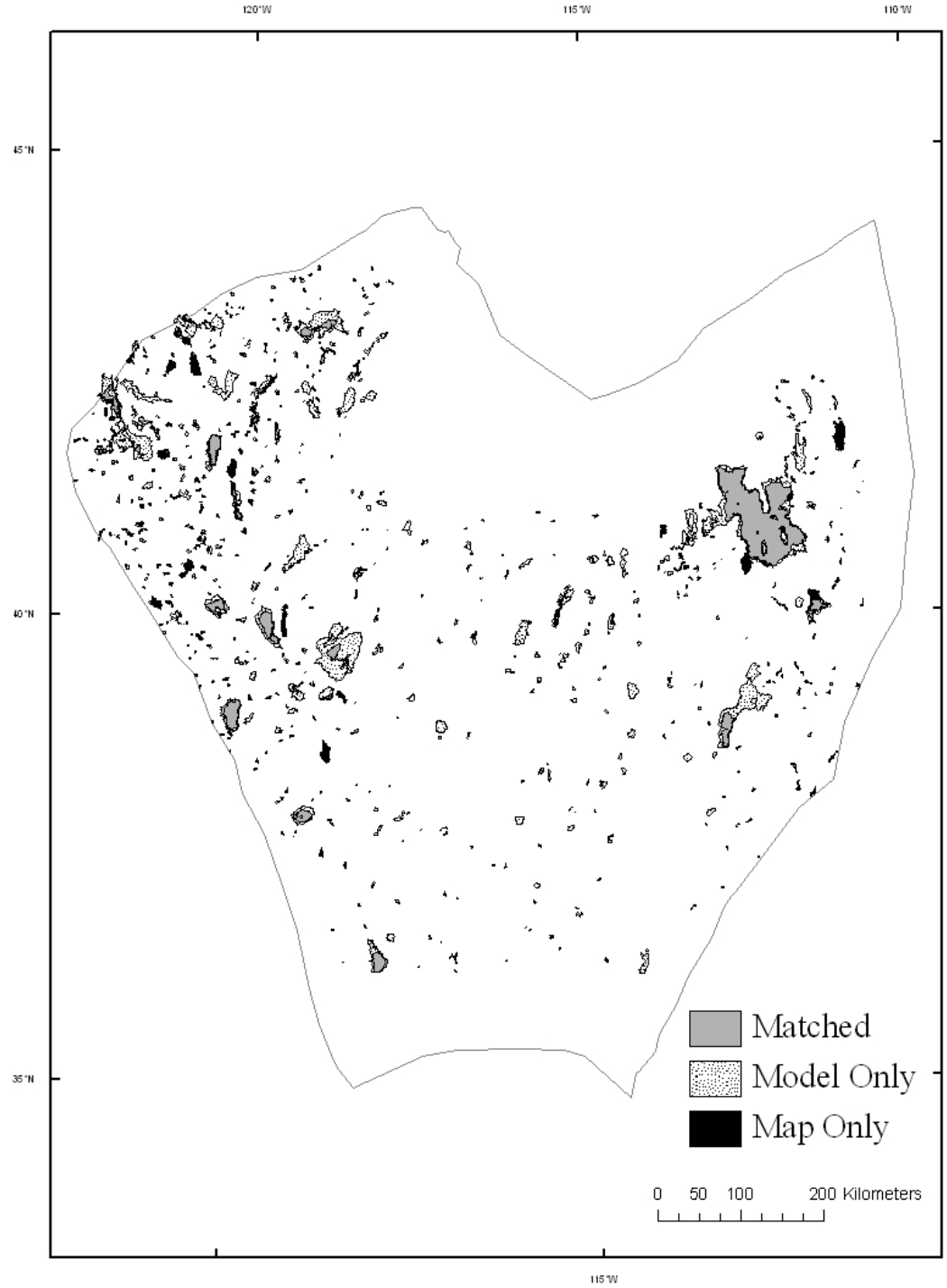

Figure 2. A map comparing mapped and simulated lake distribution under the modern condition.

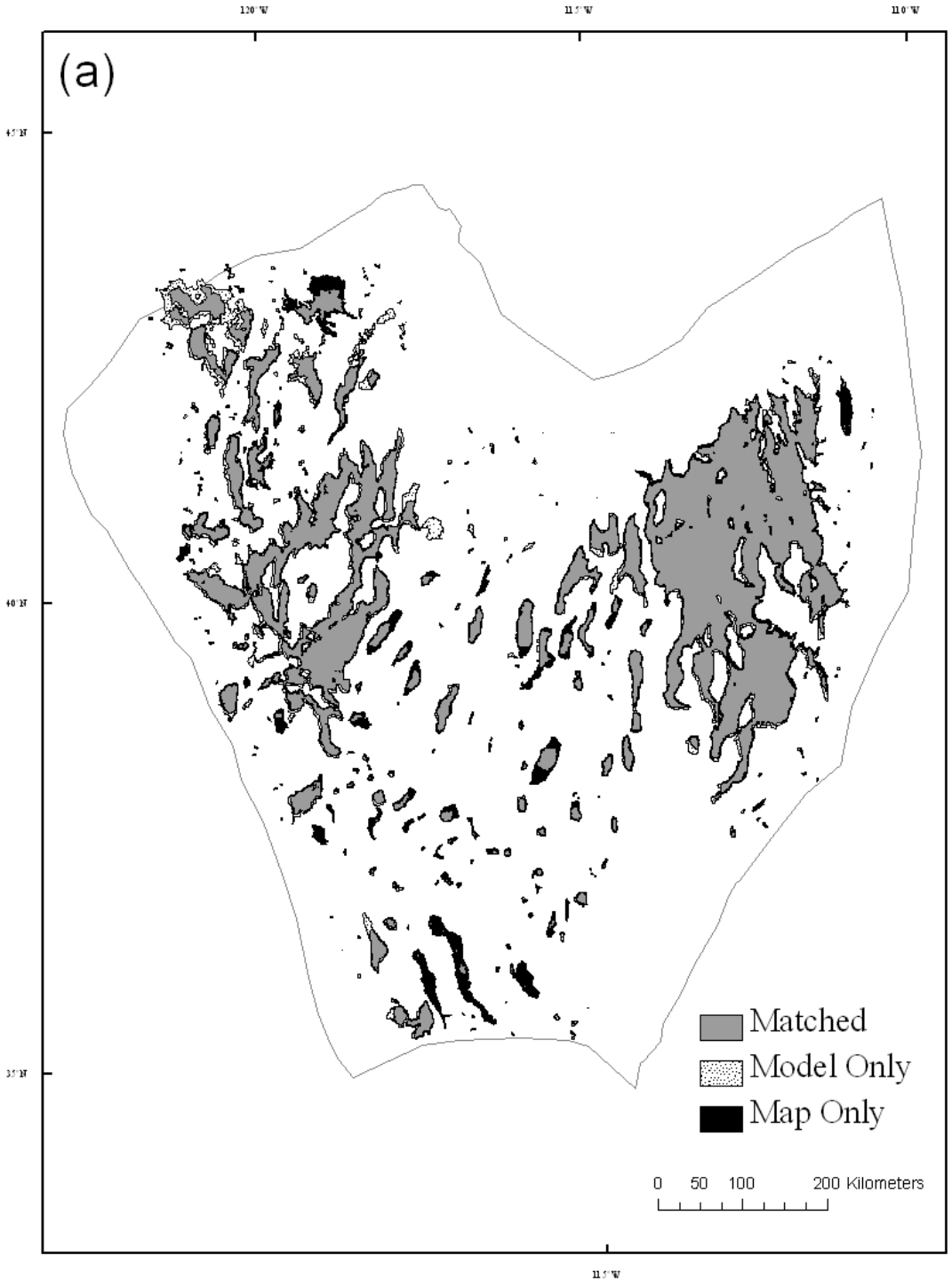
(a)
120°W
115°W
110°W
45°N
40°N
35°N
Matched
Model Only
Map Only
0 50 100 200 Kilometers

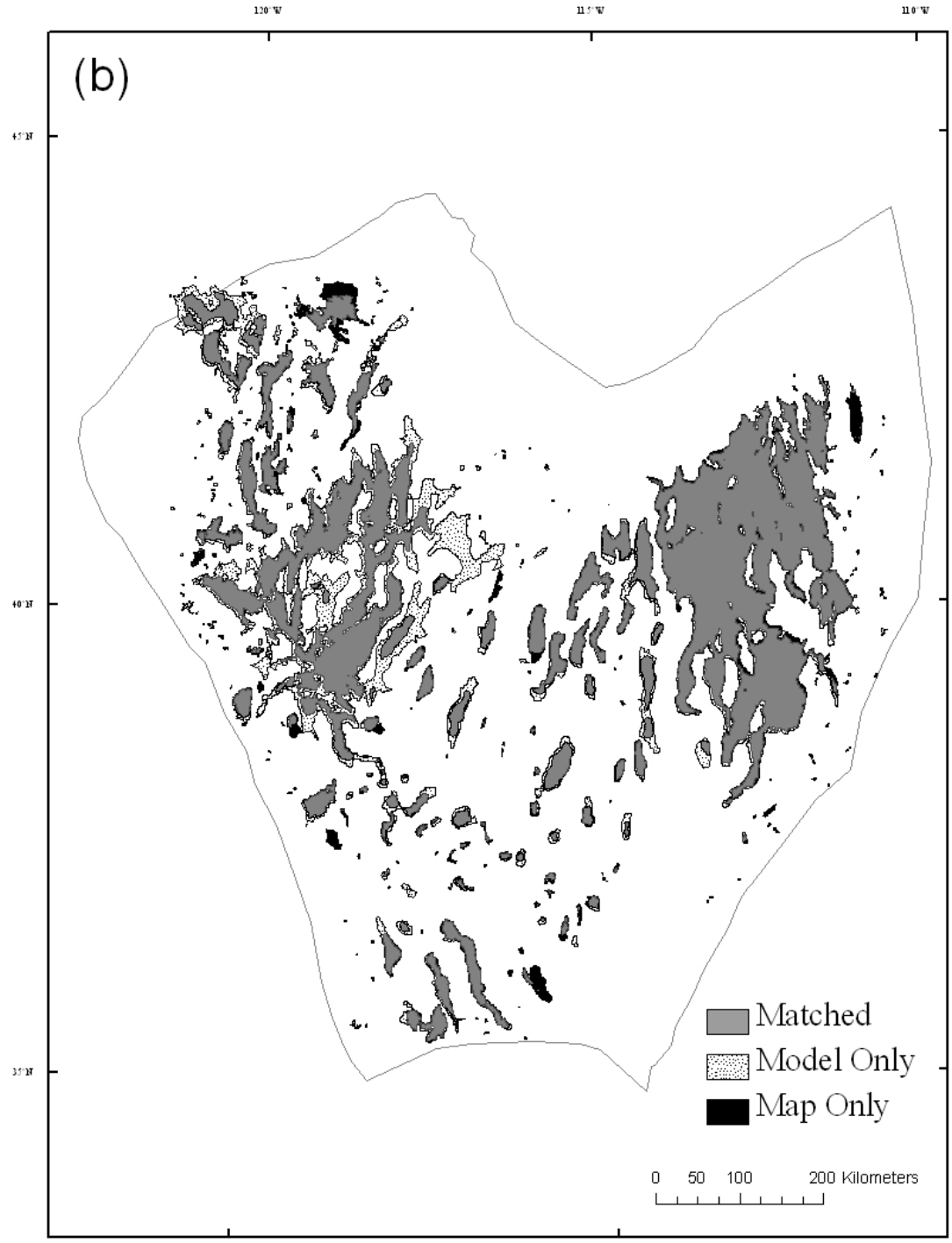

Figure 3. Maps comparing mapped and simulated lake distribution for the LGM with conditions set for (a) Lake Lahontan/ Lake Bonneville and (b) Lake Manly.

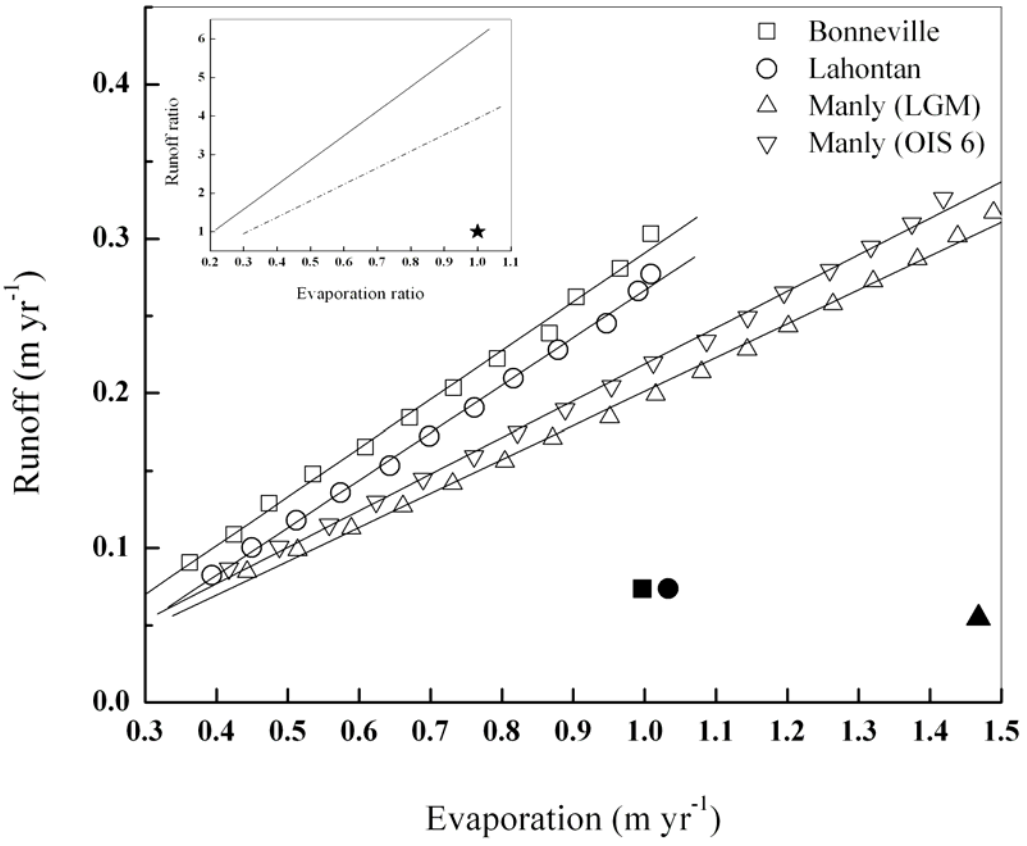

Figure 4. Possible pluvial conditions with runoff expressed as a function of evaporation for three regions. Modern conditions (filled) are plotted to show the magnitude of change required for the LGM conditions (open).

Inset: Possible pluvial conditions with runoff expressed as a function of evaporation for Bonneville (dashed) and manly (solid). Both axes are shown as a ratio of pluvial conditions to present conditions. Present condition (star) is plotted as a reference.

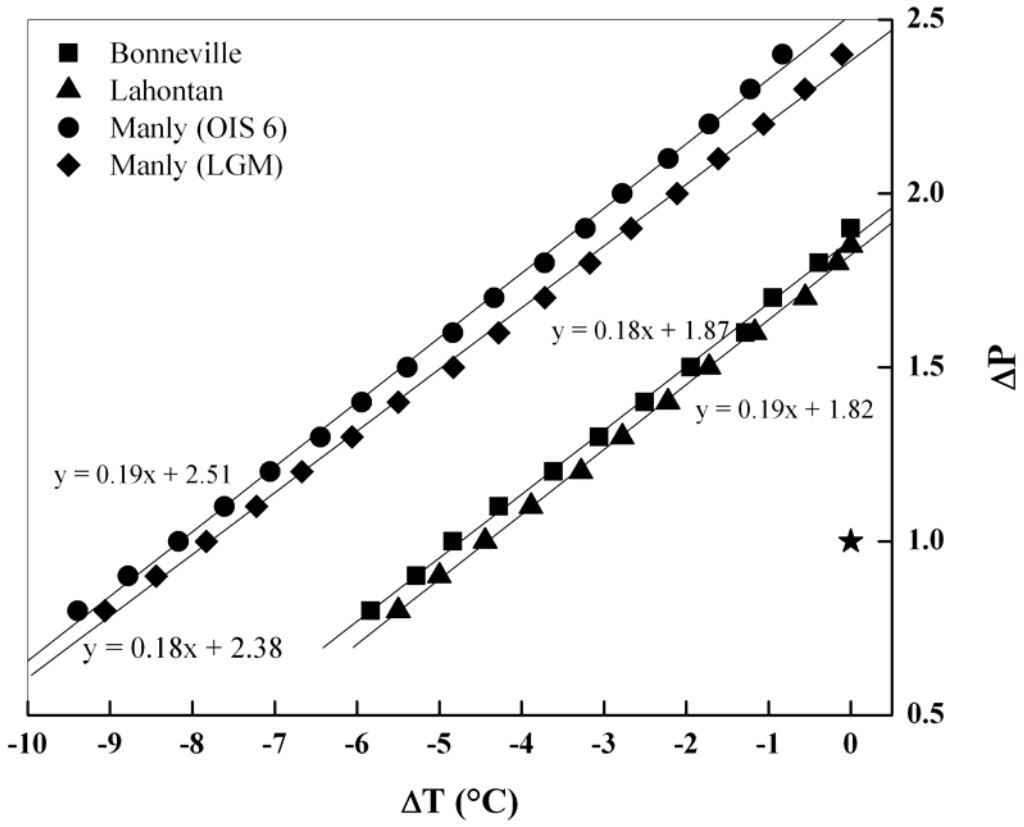

Figure 5. Possible pluvial conditions for Lake Lahontan, Bonneville, and Lake Manly regions during OIS 6 or LGM. Change in precipitation is shown as a ratio of pluvial conditions to present conditions, and temperature as a degrees change relative to the present. Modern day condition is shown as a reference (star).